Revisiting Sampson Approximations for Geometric Estimation Problems Supplementary Materials

Felix Rydell
KTH Royal Institute of Technology
felixry@kth.se

Angélica Torres
Max Planck Institute for Mathematics in the Sciences
angelica.torres@mis.mpg.de

Viktor Larsson
Lund University
viktor.larsson@math.lth.se

Overview

In this Supplementary Material, we prove more bounds related to geometric errors

$$\mathcal{E}_G^2(\boldsymbol{z}, \boldsymbol{\theta}) = \min_{\boldsymbol{\varepsilon}} \quad \|\boldsymbol{\varepsilon}\|^2 \tag{1}$$

$$\text{s.t.} \quad \boldsymbol{C}(\boldsymbol{z} + \boldsymbol{\varepsilon}, \boldsymbol{\theta}) = 0. \tag{2}$$

In Appendix A, we generalize Proposition 3.1 to the most general setting with N constraints of any degree. In Appendix B, we give a result in the spirit of Proposition 3.2 for N quadric constraints. We restrict to quadric polynomials in the case of multiple constraints (this applies to the epipolar constraints).

In Appendix C we provide details regarding the optimization of Sampson approximations, and in Appendix D we show additional results from the experiments in the main paper.

A. General Case Lower Bound for $\|\varepsilon^G\|$

In our pursuit to understand constraints of any degrees, we make use of d-norms:

$$\|\boldsymbol{x}\|_d := \sqrt[d]{x_1^d + \cdots + x_n^d}. \tag{3}$$

The 2-norm $\|\boldsymbol{x}\|_2$ is also simply denoted by $\|\boldsymbol{x}\|$. For matrices however, $\|\cdot\|$ will refer to the operator norm. We apply the following estimation of polynomials of general degrees.

Lemma A.1. *Let $q : \mathbb{R}^n \to \mathbb{R}$ be a homogeneous polynomial in n variables of degree d. Then*

$$|q(\boldsymbol{x})| \leq \mu_q \|\boldsymbol{x}\|_d^d, \tag{4}$$

where μ_q is the sum of absolute values of coefficients of q.

This lemma can be extended to non-homogeneous polynomials in a straightforward way, by replacing $\boldsymbol{x}$ by $(\boldsymbol{x}; 1)$ in (4).

Proof. Our first observation is that

$$|q(\boldsymbol{x})| \leq \big(\max_{\|\boldsymbol{y}\|_d = 1} |q(\boldsymbol{y})|\big) \|\boldsymbol{x}\|_d^d. \tag{5}$$

For $\|\boldsymbol{y}\|_d = 1$ we can bound $|q(\boldsymbol{y})|$ from above by the sum of the absolute values of the coefficients of q because, for x with $\|x\|_d = 1$, each coordinate x_i has norm ≤ 1 and therefore the norms of monomials are bounded by 1. □

We extend the notation from the main body of the paper. A set of polynomial constraints

$$\boldsymbol{C}(\boldsymbol{z}) = (C_1(\boldsymbol{z}), C_2(\boldsymbol{z}), \ \ldots, C_N(\boldsymbol{z}))^\intercal = \boldsymbol{0}, \tag{6}$$

for $\boldsymbol{z} \in \mathbb{R}^n$, can be expressed via a Taylor expansion:

$$C_i(\boldsymbol{z} + \boldsymbol{\varepsilon}) = \boldsymbol{C}(\boldsymbol{z}) + \sum_{j=1}^{d} \frac{1}{j!} \boldsymbol{\varepsilon} \times \mathcal{T}_j^{(i)}, \tag{7}$$

for each i, where $\mathcal{T}_j^{(i)}$ is a symmetric $n \times \cdots \times n$ tensor of order j, and

$$\boldsymbol{\varepsilon} \times \mathcal{T}_j^{(i)} = \sum_{l_1, \ldots, l_j \in [n]} (\mathcal{T}_j^{(i)})_{l_1, \ldots, l_j} \varepsilon_{l_1} \cdots \varepsilon_{l_j}. \tag{8}$$

For example, $\mathcal{T}_1^{(i)}$ is the Jacobian of C_i and $\mathcal{T}_2^{(i)}$ is the Hessian of C_i.

As in (8), each tensor $\mathcal{T}_j^{(i)}$ defines a polynomial, and by Lemma A.1,

$$|\boldsymbol{\varepsilon} \times \mathcal{T}_j^{(i)}| \leq \mu_j^{(i)} \|\boldsymbol{\varepsilon}\|_j^j, \tag{9}$$

where $\mu_j^{(i)}$ is the sum of absolute values of coefficients of this polynomial. Let $\boldsymbol{\varepsilon} \times \mathcal{T}_j$ denote the vector of N coordinates $(\boldsymbol{\varepsilon} \times \mathcal{T}_j^{(i)})_{i=1}^N$. Write μ_j for the sum of all $\mu_j^{(i)}$ for $i = 1, \ldots, N$, and note that

$$\|\boldsymbol{\varepsilon} \times \mathcal{T}_j\| \leq \mu_j \|\boldsymbol{\varepsilon}\|_j^j. \tag{10}$$

Recall from Section 2.2 that putting $\boldsymbol{\Sigma} = I$ gives us

$$\boldsymbol{\varepsilon}^S = -\boldsymbol{J}^\dagger \boldsymbol{C}(\boldsymbol{z}). \tag{11}$$

Proposition A.2. *Assume that the optimization problem (1) has N homogeneous constraints of at most degree d, that $\boldsymbol{J}$ evaluated at $\boldsymbol{z}$ has linearly independent rows and that $\boldsymbol{C}(\boldsymbol{z}) \in \operatorname{Im} \boldsymbol{J}$. Then*

$$\|\boldsymbol{\varepsilon}^S\| \leq \|\boldsymbol{\varepsilon}^G\| + \|\boldsymbol{J}^\dagger\| \sum_{j=2}^{d} \frac{\mu_j}{j!} \|\boldsymbol{\varepsilon}^G\|_j^j. \tag{12}$$

Recall that $\|\boldsymbol{J}^\dagger\|$ refers to the operator norm of the pseudo-inverse of $\boldsymbol{J}$.

Proof. For $\boldsymbol{\varepsilon}^G$, we have

$$0 = \boldsymbol{C}(\boldsymbol{z}) + \boldsymbol{J}\boldsymbol{\varepsilon}^G + \sum_{j=2}^{d} \frac{1}{j!} \boldsymbol{\varepsilon}^G \times \mathcal{T}_j \tag{13}$$

$$= \boldsymbol{C}(\boldsymbol{z}) + \boldsymbol{J} \left(\boldsymbol{\varepsilon}^G + \boldsymbol{J}^\dagger \sum_{j=2}^{d} \frac{1}{j!} \boldsymbol{\varepsilon}^G \times \mathcal{T}_j \right), \tag{14}$$

meaning that the norm of $\boldsymbol{\varepsilon}^S$ must be bounded from above by the norm of

$$\boldsymbol{\varepsilon}^G + \boldsymbol{J}^\dagger \sum_{j=2}^{d} \frac{1}{j!} \boldsymbol{\varepsilon}^G \times \mathcal{T}_j. \tag{15}$$

However, by (10) the statement now follows. □

B. Multiple Quadric Constraints

In this section we prove an upper bound for the geometric error in the case of multiple constraints, and take a closer look at this bound in an example with two quadric constraints. Our main tool is the following celebrated result, as stated in [3, Ch. 2, Cor. 2.15].

Theorem B.1 (Brouwer's Fixed Point Theorem)**.** *Every continuous function f from a non-empty convex compact subset K of a Euclidean space to K itself has a fixed point.*

Recall that a fixed point of a function is a point x^* in the set K such that $f(x^*) = x^*$. The main theorem of this section deals with varieties X that are a complete intersection, defined by N quadrics $\boldsymbol{C}(\boldsymbol{z}) = (C_1(\boldsymbol{z}), \ldots, C_N(\boldsymbol{z}))^\intercal$. By complete intersection, we mean that the dimension of X is $n - N$. We discuss the general case afterwards.

Define

$$\sigma_i := \text{ spectral radius of } \frac{\|\boldsymbol{J}\|}{2} (\boldsymbol{J}^\dagger)^\intercal \boldsymbol{H}_i \boldsymbol{J}^\dagger, \tag{16}$$

$$\operatorname{cond}(\boldsymbol{J}) := \|\boldsymbol{J}\| \|\boldsymbol{J}^\dagger\|. \tag{17}$$

Neither σ_i nor $\operatorname{cond}(\boldsymbol{J})$ are independent of the individual scalings of C_i for each $i = 1, \ldots, N$. They are however independent of simultaneous scaling of all constraints.

Since we will deal with multiple constraints of degree two, we first recall a classical fact about the solutions of degree 2 equations in one variable. This will be used in the proof of the main theorem.

Remark B.2. Consider the equation

$$\alpha x^2 + \beta x + \gamma = 0. \tag{18}$$

As long as $\alpha \neq 0$, the solutions to the equation are

$$x = \frac{-\beta \pm \sqrt{\beta^2 - 4\alpha\gamma}}{2\alpha}. \tag{19}$$

We can consider these solutions as a function of α, β and γ that outputs a real solution to (18) for inputs in the semi-algebraic set $\beta^2 - 4\alpha\gamma \geq 0, \alpha \neq 0$. Moreover, this function is continuous because the square root is continuous. The expression $\beta^2 - 4\alpha\gamma$ is called the discriminant of (18).

Theorem B.3. *Consider a complete intersection defined by the quadratic equations*

$$\boldsymbol{C}(\boldsymbol{z}) = (C_1(\boldsymbol{z}), C_2(\boldsymbol{z}), \ \ldots, C_N(\boldsymbol{z}))^\intercal = \boldsymbol{0}. \tag{20}$$

Assume that $\boldsymbol{J}$ is full-rank at $\boldsymbol{z}$. If a number $\kappa \geq 0$ satisfies

$$\kappa \geq \sum_{j=1}^{N} \left(\frac{|C_j(\boldsymbol{z})|}{\|\boldsymbol{J}\|} + \sigma_j \kappa \right)^2, \tag{21}$$

then

$$\|\boldsymbol{\varepsilon}^G\| \leq \operatorname{cond}(\boldsymbol{J}) \kappa. \tag{22}$$

It is easy to check if there is a κ such that the conditions (21) holds. Indeed, one solves the quadratic equation

$$\kappa = \sum_{j=1}^{N} \left(\frac{|C_j(\boldsymbol{z})|}{\|\boldsymbol{J}\|} + \sigma_j \kappa \right)^2. \tag{23}$$

If there exists real solutions, then they are ≥ 0, because the right-hand side of the equation is always non-negative. In this case, the smallest real solution is the smallest κ satisfying (21).

In order to relate theorem to the Sampson error as described in Section 2.1, we note that if the conditions of the theorem hold for $\kappa = c\|\boldsymbol{\varepsilon}^S\|/\operatorname{cond}(\boldsymbol{J})$ for some c, then $\|\boldsymbol{\varepsilon}^G\| \leq c\|\boldsymbol{\varepsilon}^S\|$.

Proof. Define

$$\varepsilon(\boldsymbol{\lambda}) := \|\boldsymbol{J}\| \boldsymbol{J}^\dagger \boldsymbol{\lambda}. \tag{24}$$

Then $f_i(\boldsymbol{\lambda}) := C_i(\boldsymbol{z} + \boldsymbol{\varepsilon}(\boldsymbol{\lambda}))/\|\boldsymbol{J}\|$ equals

$$\frac{C_i(\boldsymbol{z})}{\|\boldsymbol{J}\|} + \lambda_i + \frac{\|\boldsymbol{J}\|}{2}\boldsymbol{\lambda}^\intercal(\boldsymbol{J}^\dagger)^\intercal \boldsymbol{H}_i \boldsymbol{J}^\dagger \boldsymbol{\lambda}. \tag{25}$$

We estimate f_i from above and below using σ_i:

$$\frac{C_i(\boldsymbol{z})}{\|\boldsymbol{J}\|} + \lambda_i - \sigma_i\|\boldsymbol{\lambda}\|^2 \leq f_i(\boldsymbol{\lambda}) \leq \frac{C_i(\boldsymbol{z})}{\|\boldsymbol{J}\|} + \lambda_i + \sigma_i\|\boldsymbol{\lambda}\|^2. \tag{26}$$

This estimation can be refined for $\boldsymbol{\lambda}$ in a specific region. Indeed, let $\boldsymbol{\lambda} \in \mathbb{R}^N$ satisfy

$$\left|\lambda_i + \frac{C_i(\boldsymbol{z})}{\|\boldsymbol{J}\|}\right| \leq \sigma_i\kappa, \tag{27}$$

for each $i = 1, \ldots, N$ and let κ be as in the statement. Using the reverse triangle inequality, we have

$$|\lambda_i| \leq \frac{|C_i|}{\|\boldsymbol{J}\|} + \sigma_i\kappa, \tag{28}$$

and it follows by (21) that $\sum_{j=1}^N \lambda_j^2 \leq \kappa$.

Then from (26), we get

$$\frac{C_i(\boldsymbol{z})}{\|\boldsymbol{J}\|} + \lambda_i - \sigma_i\kappa \leq f_i(\boldsymbol{\lambda}) \leq \frac{C_i(\boldsymbol{z})}{\|\boldsymbol{J}\|} + \lambda_i + \sigma_i\kappa, \tag{29}$$

and this estimation only depends on λ_i. Fixing each $\lambda_j, j \neq i$ in (27), the solutions $\lambda_i^\pm$ to the two linear equations are

$$\lambda_i^\pm = -\frac{C_i(\boldsymbol{z})}{\|\boldsymbol{J}\|} \mp \sigma_i\kappa, \tag{30}$$

which satisfy (27). Note that by (29), for λ_i^-, $f_i(\boldsymbol{\lambda}) \geq 0$ and for λ_i^+, $f_i(\boldsymbol{\lambda}) \leq 0$. It follows that there must be a real λ_i^* such that $f_i(\boldsymbol{\lambda}) = 0$ in the interval

$$\left|\lambda_i^* + \frac{C_i(\boldsymbol{z})}{\|\boldsymbol{J}\|}\right| \leq \sigma_i\kappa, \tag{31}$$

because this interval contains both $\lambda_i^\pm$.

The existence of a real solution implies that the discriminant is greater or equal than 0 in (27) and by Remark B.2 we have that $\lambda_i^*(\hat{\boldsymbol{\lambda}}_i)$ are continuous functions (here $\hat{\boldsymbol{\lambda}}_i$ denotes the vector in $\mathbb{R}^{N-1}$ obtained by removing the i-th coordinate from $\boldsymbol{\lambda} \in \mathbb{R}^N$).

Let K be the hypercube defined in (27). In order to apply Brouwer's fixed point theorem we consider the continuous function

$$F : K \to K, \tag{32}$$

$$\boldsymbol{\lambda} \to (\lambda_1^*(\hat{\boldsymbol{\lambda}}_1), \ldots, \lambda_N^*(\hat{\boldsymbol{\lambda}}_N)). \tag{33}$$

By the theorem, there is a fixed point $\boldsymbol{\lambda}^* \in K$ with the property that $F(\boldsymbol{\lambda}^*) = \boldsymbol{\lambda}^*$. This means exactly that $(\boldsymbol{\lambda}^*)_i = \lambda_i^*(\hat{\boldsymbol{\lambda}}_i)$ for each $i = 1, \ldots, N$. By construction, $\lambda_i^*(\hat{\boldsymbol{\lambda}}_i)$ solves $f_i(\boldsymbol{\lambda}) = 0$ for fixed $\lambda_j, j \neq i$. This means that $f_i(\boldsymbol{\lambda}^*) = 0$ for each $i = 1, \ldots, N$.

To summarize, there exists a $\boldsymbol{\lambda}^* \in K$ such that $C_i(\boldsymbol{z} + \boldsymbol{\varepsilon}(\boldsymbol{\lambda}^*)) = 0$ for each $i = 1, \ldots, N$. This means that $\|\boldsymbol{\varepsilon}^G\| \leq \|\boldsymbol{\varepsilon}(\boldsymbol{\lambda}^*)\|$. Further, as we have defined $\boldsymbol{\varepsilon}$, $\|\boldsymbol{\varepsilon}(\boldsymbol{\lambda}^*)\| \leq \|\boldsymbol{J}\|\|\boldsymbol{J}^\dagger\|\|\boldsymbol{\lambda}^*\|^2$. Finally, $\|\boldsymbol{\lambda}^*\|^2 \leq \kappa$ as noted above and we are done. □

In the general case, where we are given N quadric constraints that define a variety X of dimension m that is not necessarily a complete intersection, we can use the fact that locally, it is defined by $n - m$ constraints. To be precise, the Jacobian at a generic point $\boldsymbol{x}$ of X is of rank $n - m$, and any choice of $n - m$ constraints with full-rank Jacobian locally describe X around $\boldsymbol{x}$. Heuristically, given a data point $\boldsymbol{z}$ outside the variety, we choose $n - m$ constraints for which the Jacobian has full-rank and apply Theorem B.3 to these constraints. We leave it to future work to make this rigorous.

We illustrate the theorem with an example below.

Example B.4. Consider the two quadratic constraints defining a variety in $\mathbb{R}^3$,

$$x^2 + y^2 + z^2 - 1 = 0, \tag{34}$$

$$z - xy = 0. \tag{35}$$

This curve is a complete intersection, and the associated Jacobian is

$$\boldsymbol{J} = \begin{bmatrix} 2x & 2y & 2z \\ -y & -x & 1 \end{bmatrix}. \tag{36}$$

The bound coming from Theorem B.3 can be used as long as there exists a k such that

$$\kappa \geq \sum_{j=1}^N \left(\frac{|C_j(\boldsymbol{z})|}{\|\boldsymbol{J}\|} + \sigma_j\kappa\right)^2. \tag{37}$$

Note, that this inequality will have a real solution depending on the value of $\boldsymbol{z}$. To illustrate how often this bound is satisfied, we conducted the following numerical experiment:

- We sample m data points in the curve,
- introduce an error ϵ in each point and generate a noisy sample of size m,
- for each noisy point we compute $C_i, \|J\|$ and σ_i and decide whether the inequality (21) has a solution.
- We count the percentage of points in the sample that had a positive result in the previous step.

We present our results in Figure 1

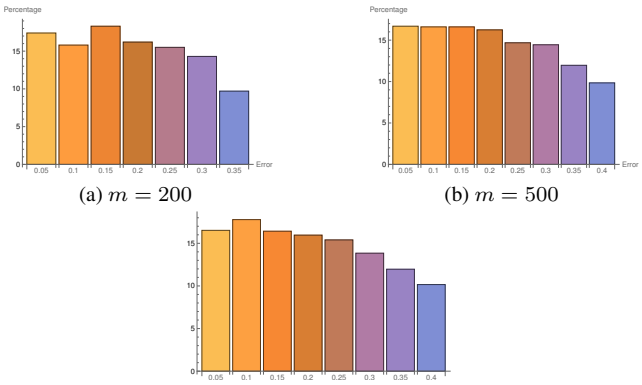

(a) $m = 200$ (b) $m = 500$ (c) $m = 1000$

Figure 1. Percentage of data points whose geometric error can be bounded using Theorem B.3. These percentages were computed over noisy samples of 200, 500 and 1000 points, and are depicted respectively in the histograms.

C. Optimization of Sampson Approximations

The constraint $C(\boldsymbol{z}, \theta)$ typically depends not only on the measurements $\boldsymbol{z}$, but also some model parameters θ which we are estimating. Fitting the parameters we want to minimize the residuals for each measurement $\boldsymbol{z}_k,\ k = 1, \ldots, m$.

$$\theta^\star = \arg\min_\theta \sum_k \|\boldsymbol{J}_k^\dagger \boldsymbol{C}(\boldsymbol{z}_k, \theta)\|^2 \tag{38}$$

where $\boldsymbol{J}_k = \frac{\partial \boldsymbol{C}(\boldsymbol{z},\theta)}{\partial \boldsymbol{z}}|_{\boldsymbol{z}=\boldsymbol{z}_k}$.

To apply standard non-linear least squares algorithms (e.g. Levenberg-Marquardt), we need to evaluate the Jacobian of the residuals $\boldsymbol{r}_k = \boldsymbol{J}_k^\dagger \boldsymbol{C}(\boldsymbol{z}_k)$ w.r.t. θ, i.e.

$$\frac{\partial \boldsymbol{r}_k}{\partial \theta} = \frac{\partial}{\partial \theta}\left((\frac{\partial \boldsymbol{C}}{\partial \boldsymbol{z}})^\dagger \boldsymbol{C}(\boldsymbol{z}, \theta) \right) \tag{39}$$

$$= \left(\frac{\partial}{\partial \theta} (\frac{\partial \boldsymbol{C}}{\partial \boldsymbol{z}})^\dagger \right) \boldsymbol{C}(\boldsymbol{z}, \theta) + (\frac{\partial \boldsymbol{C}}{\partial \boldsymbol{z}})^\dagger \frac{\partial \boldsymbol{C}}{\partial \theta} \tag{40}$$

Denote $\boldsymbol{J}_{\boldsymbol{z}} = \frac{\partial \boldsymbol{C}}{\partial \boldsymbol{z}}$ and $\boldsymbol{J}_\theta = \frac{\partial \boldsymbol{C}}{\partial \theta}$, then

$$\frac{\partial}{\partial \theta} \boldsymbol{J}_{\boldsymbol{z}}^\dagger = -\boldsymbol{J}_{\boldsymbol{z}}^\dagger \boldsymbol{J}_\theta \boldsymbol{J}_{\boldsymbol{z}}^\dagger + \boldsymbol{J}_{\boldsymbol{z}}^\dagger (\boldsymbol{J}_{\boldsymbol{z}}^\dagger)^T \boldsymbol{J}_\theta (I - \boldsymbol{J}_{\boldsymbol{z}} \boldsymbol{J}_{\boldsymbol{z}}^\dagger) \tag{41}$$

See Golub and Pereyra [2] for more details.

D. Additional Experimental Results

In Table 2 we show the full per-scene results of the covariance aware camera pose refinement from Section 4.4 in the main paper, and Table 1 show the results of refining the vanishing points using both the mid-point error and the Sampson error. For this data there was no difference in the results of the refinement.

	YUB+ [1]		NYU [5] [4]	
	Mean	AUC	Mean	AUC
VP from [6]	1.62	0.86	3.24	0.70
↳ Mid-point	1.57	0.86	3.24	0.70
↳ Sampson.	1.57	0.86	3.24	0.70

Table 1. **Refinement of vanishing points.**

References

[1] Patrick Denis, James H Elder, and Francisco J Estrada. Efficient edge-based methods for estimating manhattan frames in urban imagery. In *European Conference on Computer Vision (ECCV)*, 2008. 4

[2] Gene H Golub and Victor Pereyra. The differentiation of pseudo-inverses and nonlinear least squares problems whose variables separate. *SIAM Journal on numerical analysis*, 10(2):413–432, 1973. 4

[3] Allen Hatcher. *Algebraic topology*. Cambridge University Press, 2005. 2

[4] Florian Kluger, Eric Brachmann, Hanno Ackermann, Carsten Rother, Michael Ying Yang, and Bodo Rosenhahn. CONSAC: Robust multi-model fitting by conditional sample consensus. In *Computer Vision and Pattern Recognition (CVPR)*, 2020. 4

[5] Pushmeet Kohli Nathan Silberman, Derek Hoiem and Rob Fergus. Indoor segmentation and support inference from rgbd images. In *European Conference on Computer Vision (ECCV)*, 2012. 4

[6] Rémi Pautrat, Daniel Barath, Viktor Larsson, Martin R Oswald, and Marc Pollefeys. Deeplsd: Line segment detection and refinement with deep image gradients. In *Computer Vision and Pattern Recognition (CVPR)*, 2023. 4

τ		Chess	Fire	Heads	Office	Pumpkin	Redkitchen	Stairs	Average
5px	Reproj.	0.86 / 2.47	0.84 / 2.11	0.75 / 1.07	0.89 / 3.05	1.24 / 4.78	1.39 / 4.15	1.22 / 4.44	1.03 / 3.20
	Reproj+Cov	0.85 / 2.45	0.82 / 2.04	0.74 / 1.02	0.87 / 2.99	1.22 / 4.75	1.36 / 4.03	1.15 / 4.28	1.01 / 3.10
	↳ Sampson	0.85 / 2.45	0.82 / 2.04	0.74 / 1.02	0.87 / 2.99	1.22 / 4.74	1.36 / 4.02	1.14 / 4.27	1.01 / 3.10
10px	Reproj.	0.84 / 2.42	0.90 / 2.25	0.82 / 1.18	0.92 / 3.07	1.25 / 4.79	1.39 / 4.20	1.32 / 4.78	1.06 / 3.24
	Reproj+Cov	0.79 / 2.38	0.81 / 2.03	0.73 / 1.03	0.86 / 2.92	1.20 / 4.41	1.32 / 3.83	1.12 / 4.17	0.99 / 2.99
	↳ Sampson	0.79 / 2.37	0.81 / 2.03	0.73 / 1.03	0.86 / 2.94	1.20 / 4.40	1.32 / 3.85	1.12 / 4.20	0.98 / 2.99
20px	Reproj.	0.87 / 2.53	1.08 / 2.72	1.04 / 1.45	1.06 / 3.43	1.38 / 5.41	1.49 / 4.50	1.99 / 6.84	1.21 / 3.63
	Reproj+Cov	0.75 / 2.30	0.80 / 2.06	0.73 / 1.03	0.88 / 2.91	1.13 / 4.30	1.29 / 3.81	1.36 / 4.89	0.99 / 3.00
	↳ Sampson	0.75 / 2.31	0.80 / 2.07	0.73 / 1.03	0.88 / 2.92	1.13 / 4.34	1.29 / 3.88	1.44 / 5.25	1.00 / 3.02

Table 2. **Full results for 7Scenes**. Table shows the median rotation (deg.) and translation (cm) errors for each scene in the 7Scenes dataset for the experiment in Section 4.4 in the main paper.